RSC Advances

PAPER

View Article Online
View Journal | View Issue

Cite this: *RSC Adv.*, 2021, **11**, 9977

Removal of tetracycline hydrochloride from wastewater by Zr/Fe-MOFs/GO composites

Fuhua Wei,*[a] Qinhui Ren,[a] Huan Zhang,[a] Lili Yang,[a] Hongliang Chen,[a] Zhao Liang*[b] and Ding Chen *[b]

Received 7th February 2021
Accepted 1st March 2021

DOI: 10.1039/d1ra01027a

rsc.li/rsc-advances

Zirconium-iron metal–organic frameworks (Zr/Fe-MOFs) and Zr/Fe-MOF/graphene oxide (GO) composites were prepared *via* solvothermal synthesis using ferrous sulfate heptahydrate, zirconium acetate, and 1,3,5-benzenetricarboxylic acid. The MOFs and composites were measured using scanning electron microscopy (SEM), infrared spectrometry (IR), and thermogravimetric analysis (TGA). In this study, we explored the ability of Zr/Fe-MOFs and Zr/Fe-MOF/GO composites to adsorb tetracycline hydrochloride from an aqueous solution. Additionally, we optimized the adsorption performance by varying the ratio of MOFs and MOF composites to tetracycline hydrochloride solution, the concentration of tetracycline hydrochloride solution, and the pH of the solution. The results were investigated and fit to both pseudo-first-order and pseudo-second-order kinetic models. The results of the Freundlich and Langmuir isotherm models indicate that Zr/Fe-MOFs and Zr/Fe-MOF/GO composites have heterogeneous adsorption surfaces and that tetracycline hydrochloride is adsorbed over Zr/Fe-MOFs and Zr/Fe-MOF/GO by multilayer adsorption. Overall, our findings indicate that Zr/Fe-MOFs and Zr/Fe-MOF/GO composites can effectively treat wastewater, providing an inexpensive alternative to other methods.

1. Introduction

Antibiotics have been widely used for the treatment and prevention of bacterial infection in veterinary and human medicine, as well as in agriculture. Their abundant use as well as the ineffectiveness of traditional sewage handling methods have resulted in the accumulation of a number of antibiotics in water supplies and aquatic environments.[1] A research group at Guangzhou Institute of Geochemistry, Chinese Academy of Sciences Research Institute showed that the total usage of antibiotics in China in 2013 was about 162 000 tons, 48% of which were for human use, and the remainder were for animal use. British research suggests that failure to find a way to combat drug-resistant bacteria could lead to an extra 10 million deaths a year by 2050 with loss of $100 trillion. The UK's Antimicrobial Resistance Assessment Committee estimates that if the current situation is not improved, one million people will die as a result of this in China by 2050. Current methods for treating wastewater include photocatalytic degradation, biological treatment, advanced oxidation processes, and membrane separation.[2]

Since the 1990s, MOFs have been under intense focus in materials science research, as a result of their varying and unique structures which provide useful properties for a range of applications,[3,4] including those in energy storage,[5,6] gas storage,[7–9] catalysis,[10,11] drug delivery,[12,13] carbon dioxide capture,[14,15] magnetic properties,[16,17] and ion exchange.[18,19] A tool for the construction of lengthened porous materials has been supplied by the combination of organic linkers and metal ions.[20,21] The production of MOFs has demonstrated high sensitivity to reaction conditions. This has important ramifications for MOF synthesis since the same reagents can be used to produce different structures by varying the reaction conditions and/or methods used to prepare the compound. High-quality MOF crystals can be obtained using solvent heat or wet solution chemistry methods.[22] New approaches in preparation including microwave,[23–26] electrochemical,[27,28] and mechanochemical synthesis,[29,30] can greatly reduce synthesis time and increase production capabilities. Compared to traditional synthesis methods, constructing MOFs using the acoustic chemistry method is more concise, controllable, and convenient.[31–34]

Since graphite oxide (GO) is hydrophilic and easily dispersed in water and other polar solvents,[35] graphite oxide can also be used as an adsorbent or as a component in adsorbed composites,[36] Bandosz group[37–39] found that MOFs/GO composites have a high adsorption capacity. This is mainly due to the special dual functions of the epoxy and hydroxyl functional groups on both sides of the GO flakes, which enable them to interact with metal ions in MOFs. Therefore, MOFs/GO composites are expected to be good adsorbents for wastewater treatment.

[a]*College of Chemistry and Chemical Engineering, Anshun University, Guizhou, Anshun 561000, PR China. E-mail: wfh.1981@163.com*

[b]*State Key Laboratory of Advanced Design and Manufacturing for Vehicle Body, College of Mechanical and Vehicle Engineering, Hunan University, Changsha City, 410082, P. R. China*

For most mono-metal MOFs materials, the activity of metal sites in the structure may be masked by organic ligands or solvent molecules, leading to the failure of MOFs materials to have a good effect. Due to the good synergistic effect of bimetals, Zr and Fe were selected as metal ions and 1,3,5-benzenetricarboxylic acid as organic chains in this paper. Zr/Fe-MOFs and Zr/Fe-MOF/GO composites were synthesized with zirconium acetate and ferrous sulfate heptahydrate *via* the hydrothermal approach. Our research concluded that Zr/Fe-MOFs and Zr/Fe-MOF/GO composites can be used to successfully remove aqueous tetracycline hydrochloride.

2. Experimental

2.1 Experimental materials and instruments

The chemicals 1,3,5-benzenetricarboxylic acid (trimesic acid, $C_9H_6O_6$, H_3BTC, 98%), ferrous sulfate heptahydrate, zirconium acetate, and tetracycline hydrochloride were purchased from Aladdin Biological Technology Co., Ltd, Shanghai, China. Graphene Oxide (GO) was purchased from Beike New Material Technology Co. Ltd, Beijing, China.

We performed structural and morphological characterizations using Fourier transform infrared spectroscopy (FTIR, IRTracer-100, SHIMADZU) and field emission scanning electron microscopy (JSM-6700F, Tokyo, Japan). The thermogravimetric curves were obtained by heating the MOFs and MOF composites to 800 °C at a rate of 5 °C min^{-1} in an argon atmosphere using a NETZSCH STA 449C thermal analyzer (Selb, Germany).

2.2 Preparation of Zr/Fe-MOFs and Zr/Fe-MOFs/GO

The Zr/Fe-MOF was synthesized by combining 4.2108 g of 1,3,5-benzenetricarboxylic acid dissolved in 10 mL of ethanol, with 2.8046 g of Ferrous sulfate heptahydrate and 2.6 mL of zirconium acetate dissolved in distilled water, and stirring the solution for 30 min. Next, the prepared solution was transferred to a 50 mL reactor and reacted at 120 °C for 10 h. Once the reaction was complete, the resulting MOF was filtered and washed thoroughly with ethanol and distilled water before drying at 80 °C for 12 h in an oven. The preparation of the Zr/Fe-MOF/GO composite followed a similar method to Zr/Fe-MOFs.

2.3 Removal of tetracycline hydrochloride

Tetracycline hydrochloride was chosen as a model contaminant to evaluate the adsorption ability of the Zr/Fe-MOFs and Zr/Fe-MOF/GO composites. The adsorption of tetracycline hydrochloride was optimized by varying three variables: the concentration of tetracycline hydrochloride, the ratio of adsorbent to tetracycline hydrochloride, and the pH of tetracycline hydrochloride solution. Each experiment was conducted by adding a pre-selected quantity of adsorbent to a pre-selected concentration of tetracycline hydrochloride and stirring under ambient light. The pH was increased or decreased by adding either 0.1 M NaOH or 0.1 M HCl, respectively. The concentrations of tetracycline hydrochloride studied were 10 ppm, 20 ppm, 30 ppm, 40 ppm, and 50 ppm with 50 mg Zr/Fe-MOFs and Zr/Fe-MOF/GO composites. The ratios of adsorbent studied were 20 mg, 100 mg, and 200 mg of MOF or composite in 50 mg L^{-1} of tetracycline hydrochloride solution. Lastly, the pH was varied from 1–14 for the Zr/Fe-MOF and Zr/Fe-MOF/GO composites. To test the removal rate of tetracycline hydrochloride, each solution was monitored every hour with UV-Vis spectrophotometry to measure the absorbance at 360 nm.[40] From this, the amount of adsorbed tetracycline hydrochloride was calculated according to the following equation:

$$q_e = \frac{(C_0 - C_e)V}{m} \quad (1)$$

where C_0, C_e, V, and m are the initial concentrations of the solution (ppm), equilibrium concentrations of the solution (ppm), the volume of the solution (L), and the mass of the adsorbent (g), respectively.

3. Results and discussion

As shown in Fig. 1, the Fourier transform infrared spectroscopy spectrum showed characteristic peaks of the Zr/Fe-MOFs at 1569 cm^{-1} and 1380 cm^{-1} and Zr/Fe-MOF/GO at 1572 cm^{-1} and 1382 cm^{-1}, respectively. Because of the existence of carboxyl, no peak appeared at 1710 cm^{-1} where a strong carbonyl peak would be expected.[41] This is primarily due to the extended conjugate π-bonds of the carboxylate which form from the carboxyl anion to make the two oxygen atom equivalents. Hence, the density of the electron cloud between atoms is distributed symmetrically.

The morphology of the MOFs was observed using SEM, as exhibited in Fig. 2. The result showed the unusual morphology and high dispersibility of the MOFs crystals. The molecular interaction of the organic ligand was weakened or even vanished, and the deprotonation of the organic ligand was enhanced, which promoted the growth of crystallite in aqueous solution. The irregular morphology observed in Fig. 2(a) was mainly caused by the inconsistent coordination ability between the two metal ions and the organic chain. As shown in Fig. 2(b), the MOF's irregular morphology could not be displayed due to the presence of GO in the composite material, which pasted MOFs together to form.

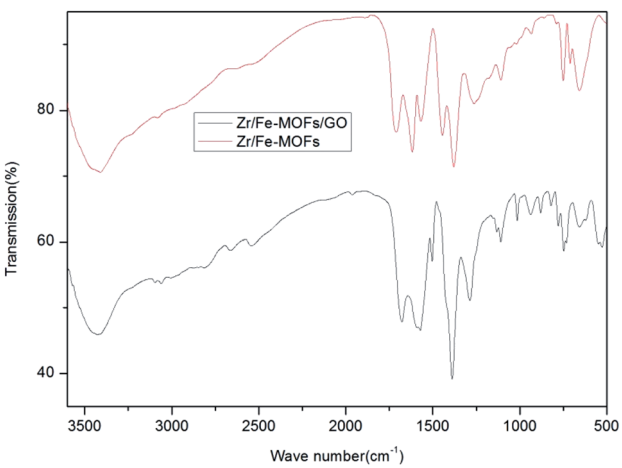

Fig. 1 IR of MOFs.

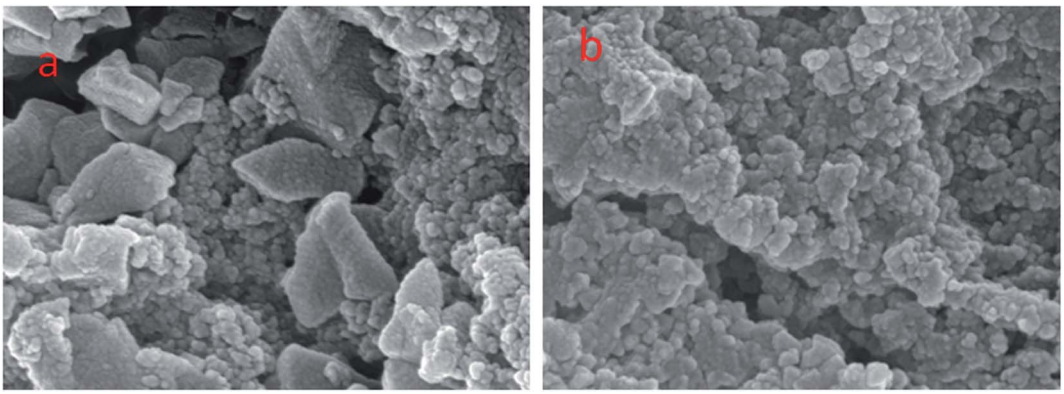

Fig. 2 (a and b) SEM of MOFs.

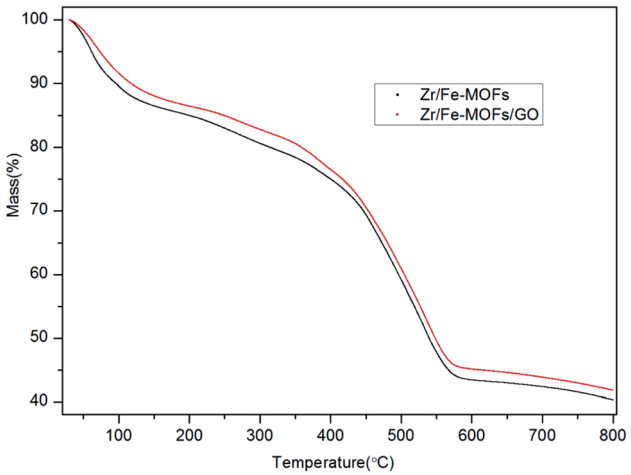

Fig. 3 TG of MOFs.

The thermogravimetric analysis (TGA) curves for the Zr/Fe-MOF and Zr/Fe-MOF/GO composites exhibit three steps, as shown in Fig. 3. The first step occurs between 20 °C and 134 °C for the plain MOF and 20 °C and 140 °C for the composite and indicates mass loss of 12.9% and 10.9%, respectively. This is likely attributed to the evaporation of water molecules from the sample. The second step occurs between 134 °C and 384 °C for the plain MOF and 140 °C and 346 °C for the composite, accounting for 10.9% and 7.9% loss, respectively, which can be attributed to the oxidation of Fe^{2+}.[42] The third step occurs between 384 °C and 587 °C for the plain MOF and 346 °C and 572 °C for the composite and indicates the temperature at which the structure and organic linker of MOFs are destroyed. From this, it can be concluded that the thermal stability of the MOF and composite is 384 °C and 346 °C, respectively. The final residue of each was 43.6% and 45.9% of the original, respectively.

In order to study the impact of the concentration of tetracycline hydrochloride on its removal, we tested the removal at concentrations of 20 mg L^{-1}, 30 mg L^{-1}, 40 mg L^{-1}, and 50 mg L^{-1} tetracycline hydrochloride solution, while consistently using 50 mg of Zr/Fe-MOFs or Zr/Fe-MOF/GO composites. First, Zr/Fe-MOFs and Zr/Fe-MOF/GO precipitate and accumulate under the addition of a large number of MOFs, thus reducing the production of active substances in the removal process.[43] Second, there is competition among tetracycline hydrochloride molecules for active sites on the MOFs and MOF composites, which is especially important because tetracycline hydrochloride molecules can produce other intermediates in the adsorption process.[44]

Fig. 4 shows that the removal efficiencies of tetracycline hydrochloride by the Zr/Fe-MOFs reached 56.1%, 60.8%, 62.8%, 69.6%, and 84.9% at 50 mg L^{-1}, 40 mg L^{-1}, 30 mg L^{-1}, 20 mg L^{-1}, and 10 mg L^{-1}, respectively and Zr/Fe-MOF/GO

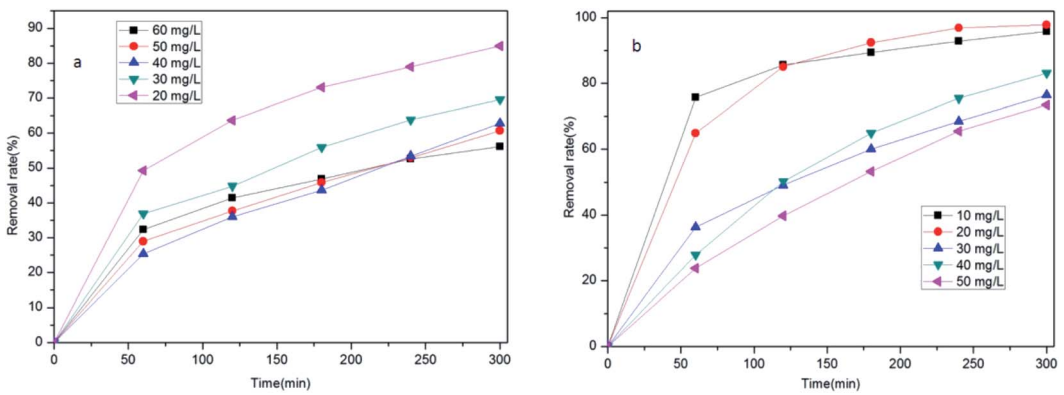

Fig. 4 Removal rates of tetracycline hydrochloride (a Zr/Fe-MOFs; b Zr/Fe-MOFs/GO).

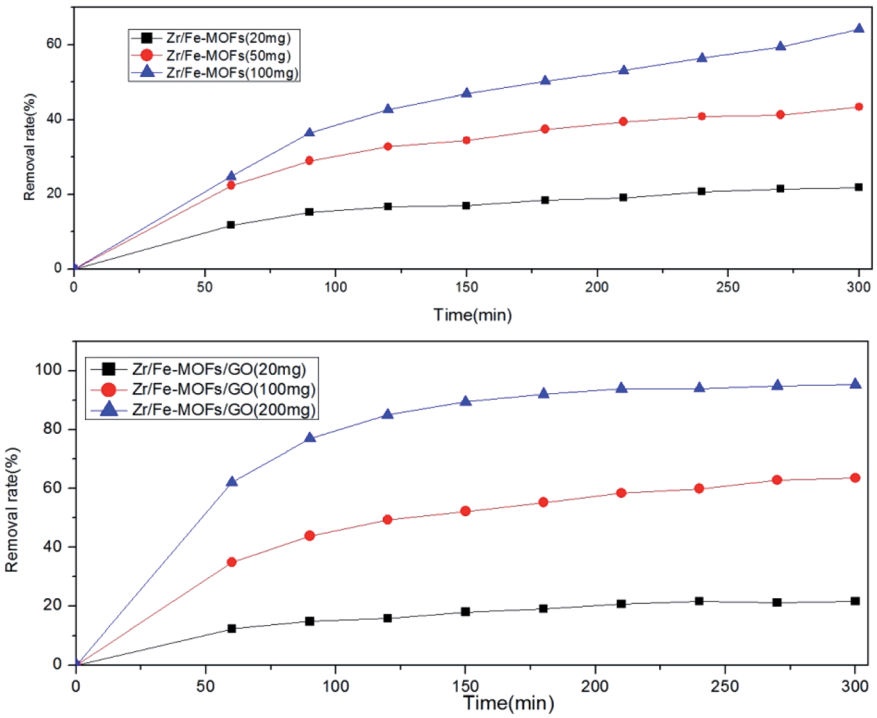

Fig. 5 The removal efficiencies of different doses of MOFs on tetracycline hydrochloride.

composites reached 73.5%, 83.1%, 76.4%, 97.8%, and 95.9% at 60 mg L^{-1}, 50 mg L^{-1}, 40 mg L^{-1}, 30 mg L^{-1}, and 20 mg L^{-1}, respectively. With the increase of adsorption time, the adsorption active sites of Zr/Fe-MOFs and Zr/Fe-MOF/GO materials reached saturation, the linearity became flat, and the removal rate might be in the intersection position. The results revealed the superior performance of the composites over the MOFs. They also revealed that as concentration decreases, the efficiencies increase. The results clearly show that Zr/Fe-MOFs and Zr/Fe-MOF/GO have great potential for tetracycline hydrochloride adsorption at relatively low concentrations.

In addition to the concentration of the pollutant, the ratio of adsorbent to pollutant affects the efficiency of treatment. To study this effect, Fig. 5 shows the removal efficiencies of tetracycline hydrochloride of Zr/Fe-MOFs and Zr/Fe-MOFs/GO composites in 50 mg L^{-1} of tetracycline hydrochloride. The removal rates were 21.2%, 56.5%, and 83.7% and 21.6%, 64.2%, and 95.3%, respectively. The positive correlation between dosage and removal rate can be attributed to an increase in active sites available. Whereas the 20 mg study did not produce significant differences between the two adsorbent materials, the 100 mg and 200 mg studies did show superior performance of the composite material over the plain MOF material. A control study was conducted to test the effectiveness of GO without a MOF, in which the same quantities of GO were tested with 50 mg L^{-1} tetracycline hydrochloride for 12 h. The removal rate for all three was found to be 5.3%, indicating that the combination of GO and MOFs was superior for removing tetracycline hydrochloride.

A major contributor to the adsorption of tetracycline hydrochloride by Zr/Fe-MOF/GO is the π–π interactions and hydrogen bonding.[45–47] Additionally, since the amine group of the tetracycline hydrochloride molecule is basic, the chemisorption mechanism relies heavily on acid–base interactions. Therefore, this study tested the effect of pH on the adsorption performance. The results, shown in Fig. 6, indicate that pH greatly affects the adsorption performance; the adsorption capacity initially increased with increasing pH, with a peak at pH = 7 before decreasing as the pH of the solution continued to rise. This phenomenon can be attributed to the presence of electric charges in three forms of tetracycline hydrochloride molecules and electrostatic interactions that dominate in the

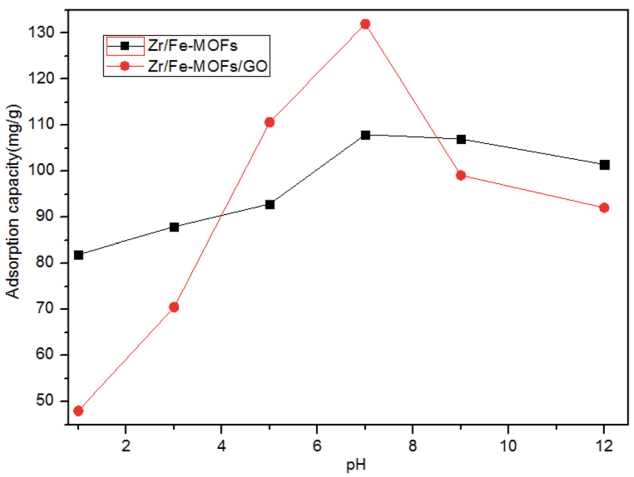

Fig. 6 Effect of pH on the adsorption amount of tetracycline hydrochloride.

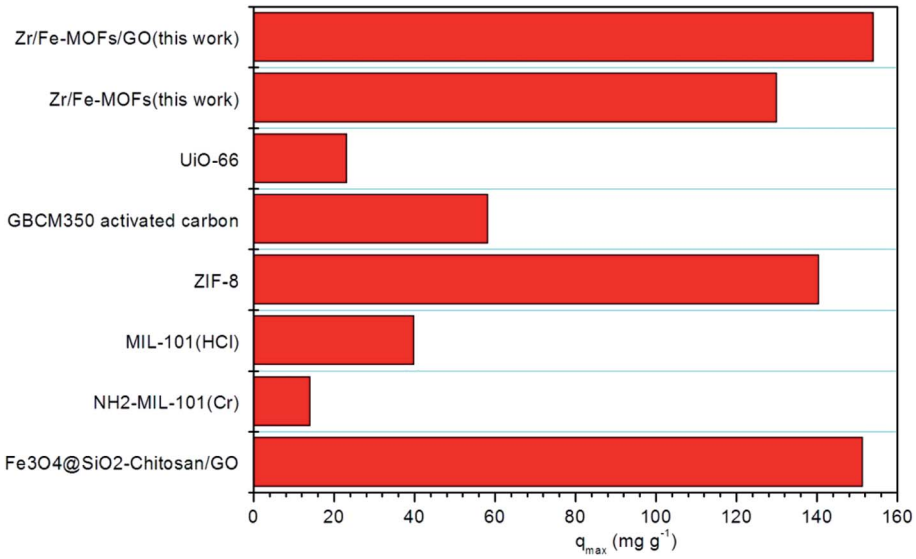

Fig. 7 Comparison of the Zr/Fe-MOFs and Zr/Fe-MOFs/GO adsorbent with other materials on TC.

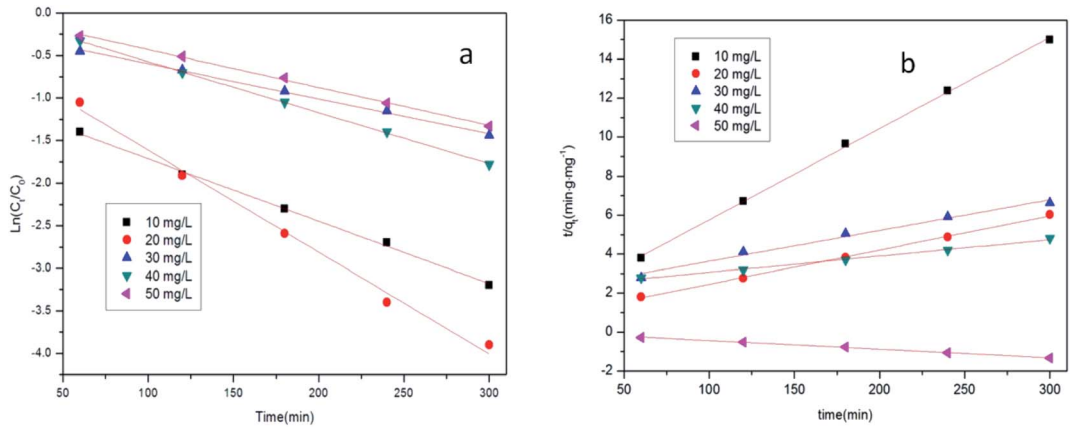

Fig. 8 Kinetic model analysis of Zr/Fe-MOFs/GO (a the pseudo-first order model; b the pseudo-second order model).

adsorption process.[48] In addition, the adsorption capacity of Zr/Fe-MOF/GO and Zr/Fe-MOFs composites in the pH range of 5–9 had no significant effect, suggesting that the effect of interaction was responsible for the tetracycline hydrochloride adsorption process.

To decrease the expense of this technique, the MOFs and MOF composites should ideally be reusable. The Zr/Fe-MOFs and Zr/Fe-MOF/GO composites were used for multiple cycles to determine their reusability. Between each cycle, the MOFs and composites were rinsed and stirred in distilled water for 5 h before being filtered and dried. The results showed that after three cycles, the decrease of Zr/Fe-MOFs and Zr/Fe-MOF/GO activity was only 25% and 31%, respectively and that after 5 cycles, the activity was decreased by 59% and 67%, respectively, indicating reasonable reusability.

Lastly, the results of tetracycline hydrochloride removal by Zr/Fe-MOFs and Zr/Fe-MOF/GO composites were compared to that of Fe_3O_4@SiO_2-chitosan/GO,[43] NH_2-MIL-101(Cr),[49] MIL-101(HCl),[50] ZIF-8,[51] GBCM350 activated carbon,[52] and Uio-66 (ref. 53) adsorbents, as shown in Fig. 7. The Zr/Fe-MOFs and Zr/Fe-MOF/GO clearly show superior performance to other adsorbents.

To fully understand and study the kinetics of Zr/Fe-MOF/GO composite adsorption of tetracycline hydrochloride, the optimum conditions of each test were analyzed. In accordance with reports in the literature, the removal of contaminants was described by the following kinetic models.[54–56]

The Pseudo-first-order kinetic model:

Table 1 Parameters of the process of tetracycline adsorption by Zr/Fe-MOFs/GO

	Pseudo-first order		Pseudo-second order	
Concentration	K	R^2	K	R^2
10 mg L^{-1}	0.01500	0.9973	−0.004450	0.9977
20 mg L^{-1}	0.006000	0.9911	0.008330	0.9936
30 mg L^{-1}	0.004100	0.9970	0.01575	0.9818
40 mg L^{-1}	0.01198	0.9997	0.01753	0.9985
50 mg L^{-1}	0.007330	0.9977	0.04677	0.9991

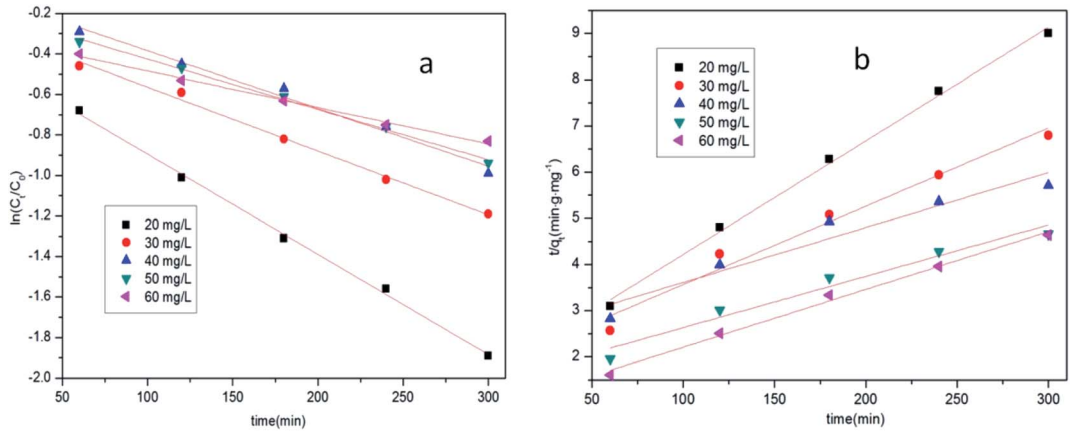

Fig. 9 Kinetic model analysis of Zr/Fe-MOFs (a the pseudo-first order model; b the pseudo-second order model).

Table 2 Parameters of the process of tetracycline adsorption by Zr/Fe-MOFs

	Pseudo-first order		Pseudo-second order	
Concentration	K	R^2	K	R^2
60 mg L^{-1}	0.004950	0.9927	−0.01252	0.9920
50 mg L^{-1}	0.003150	0.9946	0.01112	0.9543
40 mg L^{-1}	0.002850	0.9817	0.01108	0.9179
30 mg L^{-1}	0.002480	0.9922	0.01695	0.9678
20 mg L^{-1}	0.001800	0.9974	0.02458	0.9962

$$\ln\frac{C_t}{C_0} = -k_1 t \quad (2)$$

The Pseudo-second-order kinetic model:

$$\frac{t}{q_t} = \frac{t}{q_e} + \frac{1}{k_2 q_e^2} \quad (3)$$

In these equations, C_t, C_0, k_1, k_2, and t are the concentration of tetracycline hydrochloride at time t, the initial concentration of tetracycline hydrochloride, the kinetics reaction rate constant (min^{-1}), and the reaction time (min), respectively. The variables q_t and q_e represent the amounts (mg g^{-1}) of the adsorbents at time t and equilibrium, respectively. The results of Zr/Fe-MOF/GO composite calculations are presented in Fig. 8 and Table 1. For each test, the correlation coefficient R^2 was greater than 0.99, except for the pseudo-second-order model with tetracycline hydrochloride at 30 mg L^{-1}, which had an R^2 value of 0.98. The results indicate that both the pseudo-first-order model and pseudo-second-order model are appropriate for describing the removal of tetracycline hydrochloride. The first kinetic model is more suitable to describe the adsorption of Zr/Fe-MOFs/GO for tetracycline hydrochloride.

The test results are compared and fit to a kinetic model, as shown in Fig. 9 and Table 2. The correlation coefficient R^2 of the pseudo-first-order model was larger than that of the pseudo-second-order model, indicating that the first kinetic model is more suitable for describing the adsorption of tetracycline hydrochloride by the MOF composites. It can be seen from Fig. 8, 9, Tables 1 and 2 that kinetics is more suitable for describing the adsorption of tetracycline hydrochloride by MOF composites than by plain MOFs.

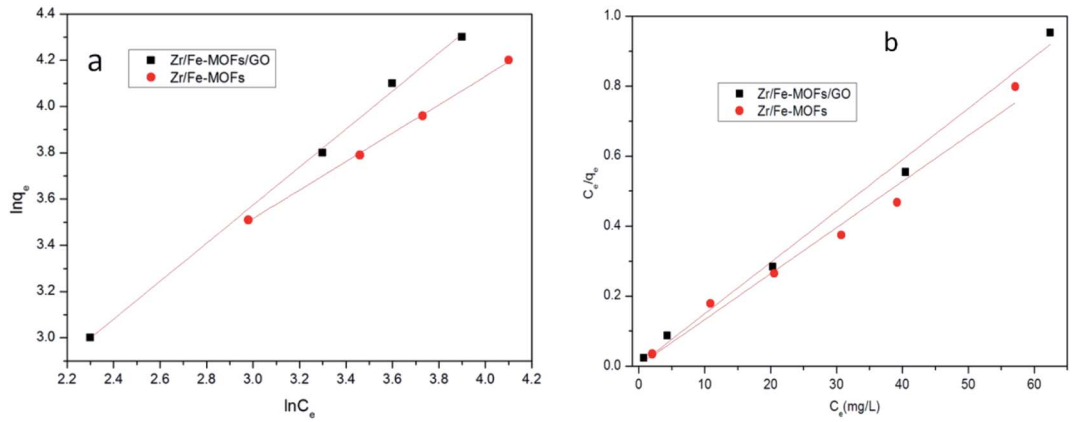

Fig. 10 Adsorption isotherms for tetracycline hydrochloride over Zr/Fe-MOFs and Zr/Fe-MOFs/GO (a Freundlich plots of the isotherms; b Langmuir of the isotherms).

Table 3 Langmuir and Freundlich isotherms parameters for CR adsorption over GO/MOFs

	Langmuir adsorption isotherm			Freundlich adsorption isotherm		
	K (L mg^{-1})	Q_0 (mg g^{-1})	R^2	K_f (mg g^{-1} (L mg^{-1})$^{1/n}$)	n	R^2
Zr/Fe-MOFs/GO	9.270	760	0.9913	5.305	1.624	0.9988
Zr/Fe-MOFs	4.910	681	0.9759	3.027	1.216	0.9974

To describe the adsorption isotherm more scientifically, the Freundlich and Langmuir isotherm model was used to analyze the relationship between the equilibrium concentration of tetracycline hydrochloride and its adsorption quantity in an aqueous solution.[57] The equations are:

$$\ln k_f = \ln q_e - \frac{1}{n}\ln C_e \quad (4)$$

$$\frac{C_e}{q_e} = \frac{C_e}{q_m} + \frac{1}{k_L q_m} \quad (5)$$

where n and k_f (mg g^{-1}) are the Freundlich constants related to intensity and the adsorption capacity, respectively.

The adsorption isotherms were obtained after adsorption for 5 h and are shown in Fig. 10 and Table 3. The adsorption of tetracycline hydrochloride onto Zr/Fe-MOFs and Zr/Fe-MOF/GO composites could be accurately described by the Freundlich and Langmuir model with R^2-values of 0.9974 and 0.9988, respectively. Additionally, both $1/n$ values were less than 1, at 0.8221 and 0.6157, respectively, indicating that Zr/Fe-MOFs and Zr/Fe-MOF/GO composites have heterogeneous adsorption surfaces and that Zr/Fe-MOFs and Zr/Fe-MOF/GO composites conduct multilayer adsorption of tetracycline hydrochloride.

4. Conclusions

Zr/Fe-MOFs and Zr/Fe-MOF/GO composites were prepared by hydrothermal methods to test their effectiveness in tetracycline hydrochloride cleanup. The study tested the impact of the concentration of tetracycline hydrochloride, the ratio of adsorbent to tetracycline hydrochloride, and the pH of tetracycline hydrochloride solution on the effectiveness of adsorption. The adsorption of tetracycline hydrochloride was analyzed with the pseudo-first-order model and the pseudo-second-order model. It can be seen from the results that both the pseudo-first-order model and the pseudo-second-order model are suitable for describing the removal of tetracycline hydrochloride by Zr/Fe-MOFs and ZR/Fe-MOF/GO, but the pseudo-first-order model is better than the pseudo-second-order model. Adsorption isotherms for tetracycline hydrochloride over Zr/Fe-MOFs and Zr/Fe-MOFs/GO were analyzed with the Freundlich and Langmuir model, respectively. The results indicated that Zr/Fe-MOFs and Zr/Fe-MOF/GO composites have heterogeneous adsorption surfaces and multilayer adsorption of tetracycline hydrochloride. The results showed that Zr/Fe-MOFs and Zr/Fe-MOF/GO composites could effectively remove tetracycline hydrochloride, indicating the application potential of MOF and MOF composite.

Conflicts of interest

There are no conflicts to declare.

Acknowledgements

The project was supported by Guizhou Education Department Youth Science and Technology Talents Growth Project (KY [2019]149).

References

1 Liu, Y. Zhang, M. Yang, Z. Tian, L. R. Ren and S. J. Zhang, *Environ. Sci. Technol.*, 2012, **46**, 7551–7557.
2 I. Michael, L. Rizzo, C. S. McArdell, C. M. Manaia, C. Merlin, T. Schwartz, C. Dagot and D. Fatta-Kassinos, *Water Res.*, 2013, **47**, 957–995.
3 H. Sato, W. Kosaka, R. Matsuda, A. Hori, Y. Hijikata, R. V. Belosludov, S. Sakaki, M. Takata and S. Kitagawa, *Science*, 2013, **343**, 167–170.
4 H. Wang, J. Xu, D. S. Zhang, Q. Chen, R. M. Wen, Z. Chang and X. H. Bu, *Angew. Chem., Int. Ed.*, 2015, **54**, 5966–5970.
5 W. Xia, A. Mahmood, R. Q. Zou and Q. Xu, *Energy Environ. Sci.*, 2015, **8**, 1837–1866.
6 L. Wang, Y. Z. Han, X. Feng, J. W. Zhou, P. F. Qi and B. Wang, *Coord. Chem. Rev.*, 2016, **307**, 361–381.
7 Yuan, D. Zhao, D. F. Sun and H. C. Zhou, *Angew. Chem., Int. Ed.*, 2010, **49**, 5357–5361.
8 Y. B. He, W. Zhou, G. D. Qian and B. L. Chen, *Chem. Soc. Rev.*, 2014, **43**, 5657–5678.
9 Y. Yan, M. Juricek, F. X. Coudert, N. A. Vermeulen, S. Grunder, A. Dailly, W. Lewis, A. J. Blake, J. F. Stoddart and M. Schroder, *J. Am. Chem. Soc.*, 2016, **138**, 3371–3381.
10 C. C. Wang, J. R. Li, X. L. Lv, Y. Q. Zhang and G. S. Guo, *Energy Environ. Sci.*, 2014, **7**, 2831–2867.
11 J. Della Rocca, D. M. Liu and W. B. Lin, *Acc. Chem. Res.*, 2011, **44**, 957–968.
12 C. Y. Sun, C. Qin, X. L. Wang and Z. M. Su, *Expert Opin. Drug Delivery*, 2013, **10**, 89–101.
13 A. R. Millward and O. M. Yaghi, *J. Am. Chem. Soc.*, 2005, **127**, 17998–17999.
14 K. Sumida, D. L. Rogow, J. A. Mason, T. M. McDonald, E. D. Bloch, Z. R. Herm, T. H. Bae and J. R. Long, *Chem. Rev.*, 2012, **112**, 724–781.
15 L. E. Kreno, K. Leong, O. K. Farha, M. Allendorf, R. P. Van Duyne and J. T. Hupp, *Chem. Rev.*, 2012, **112**, 1105–1125.
16 H. Ogawa, K. Mori, K. urashima, S. Karasawa and N. Koga, *Inorg. Chem.*, 2016, **55**, 717–728.

17 X. Y. Liu, X. N. Qu, S. Zhang, H. S. Ke, Q. Yang, Q. Shi, Q. Wei, G. Xie and S. P. Chen, *Inorg. Chem.*, 2015, **54**, 11520–11525.
18 M. Lalonde, W. Bury, O. Karagiaridi, Z. Brown, J. T. Hupp and O. K. Farha, *J. Mater. Chem. A*, 2013, **1**, 5453–5468.
19 L. Gao, C. Y. Li and K. Y. Chan, *Chem. Mater.*, 2015, **27**, 3601–3608.
20 B. Moulton and M. J. Zaworotko, *Chem. Rev.*, 2001, **101**, 1629–1658.
21 O. Delgado-Friedrichs, M. O'Keeffe and O. M. Yaghi, *Phys. Chem. Chem. Phys.*, 2007, **9**, 1035–1043.
22 A. U. Czaja, N. Trukhan and U. Muller, *Chem. Soc. Rev.*, 2009, **38**, 1284–1293.
23 L. Hashemi and A. Morsali, *CrystEngComm*, 2012, **14**, 779–781.
24 J. Klinowski, F. A. Almeida Paz, P. Silva and J. Rocha, *Dalton Trans.*, 2011, **40**, 321–330.
25 Z. Ni and R. I. Masel, *J. Am. Chem. Soc.*, 2006, **128**, 12394–12395.
26 S. H. Jhung, J. H. Lee, P. M. Forster, G. Ferey, A. K. Cheetham and J. S. Chang, *Chem.–Eur. J.*, 2006, **12**, 7899–7905.
27 A. Martinez Joaristi, J. Juan-Alcãniz, P. Serra-Crespo, F. Kapteijn and J. Gascon, *Cryst. Growth Des.*, 2012, **12**, 3489–3498.
28 U. Mueller, M. Schubert, F. Teich, H. Puetter, K. Schierle-Arndt and J. Pastre, *J. Mater. Chem.*, 2006, **16**, 626–636.
29 S. L. James, C. J. Adams, C. Bolm, D. Braga, P. Collier, T. Friscic, F. Grepioni, K. D. M. Harris, G. Hyett, W. Jones, A. Krebs, J. Mack, L. Maini, A. G. Orpen, I. P. Parkin, W. C. Shearouse, J. W. Steed and D. C. Waddell, *Chem. Soc. Rev.*, 2012, **41**, 413–447.
30 H. Sakamoto, R. Matsuda and S. Kitagawa, *Dalton Trans.*, 2012, **41**, 3956–3961.
31 N. Stock and S. Biswas, *Chem. Rev.*, 2012, **112**, 933–969.
32 G. Luo, D. Wu, L. Liu, D. X. Li, Q. H. Zhao, Z. J. Xiao and J. C. Dai, *Sci. China Chem.*, 2012, **55**, 1213–1219.
33 M. Bera, A. Rana, D. S. Chowdhuri, D. Hazari, S. K. Jana, H. Puschmann and S. Dalai, *J. Inorg. Organomet. Polym. Mater.*, 2012, **22**, 897–902.
34 Y. C. Chuang, W. L. Ho, C. F. Sheu, G. H. Lee and Y. Wang, *Chem. Commun.*, 2012, **48**, 10769–10771.
35 S. Park, J. An, I. Jung, R. D. Piner, S. J. An, X. Li, A. Velamakanni and R. S. Ruoff, *Nano Lett.*, 2009, **9**, 1593.
36 K. C. Kemp, H. Seema, M. Saleh, N. n. H. Le, K. Mahesh, V. Chandra and K. S. Kim, *Nanoscale*, 2013, **5**, 3149.
37 C. Petit and T. J. Bandosz, *Adv. Mater.*, 2009, **21**, 4753.
38 C. Petit and T. J. Bandosz, *Dalton Trans.*, 2012, **41**, 4027.
39 C. Petit and T. J. Bandosz, *J. Mater. Chem.*, 2009, **19**, 6521.
40 H. Wang, X. Yuan, Y. Wu, G. M. Zeng, H. R. Dong, X. H. Chen, L. J. Leng, Z. B. Wu and L. J. Peng, *Appl. Catal., B*, 2016, **186**, 19–29.
41 C. I. Ezugwu, M. A. Asraf, X. Li, S. W. Liu, C. M. Kao, S. F. Zhuiykov and F. Verpoort, *J. Colloid Interface Sci.*, 2018, **519**, 214–223.
42 F. H. Wei, D. Chen, Z. Lang, S. Q. Zhao and Y. Luo, *RSC Adv.*, 2017, **7**, 46520–46528.
43 B. Huang, Y. Liu, B. Li, S. B. Liu, G. M. Zeng, Z. W. Zeng, X. H. Wang, Q. M. Ning, B. H. Zheng and C. P. Yang, *Carbohydr. Polym.*, 2017, **157**, 576.
44 F. Chen, Q. Yang, X. Li, G. M. Zeng, D. B. Wang, C. G. Niu, J. W. Zhao, H. X. An, T. Xie and Y. C. Deng, *Appl. Catal., B*, 2017, **200**, 330–342.
45 N. Tian, Q. M. Jia, H. Y. Su, Y. F. Zhi, A. H. Ma, J. Wu and S. Y. Shan, *J. Porous Mater.*, 2016, **23**, 1–10.
46 T. Hu, H. Lv, S. Shan, Q. M. Jia, H. Y. Su, N. Tian and S. C. He, *RSC Adv.*, 2016, **6**, 73741–73747.
47 C. S. Wu, Z. H. Xiong, C. Li and J. M. Zhang, *RSC Adv.*, 2015, **5**, 82127–82137.
48 S. Alvarez-Torrellas, R. S. Ribeiro, H. T. Gomes, G. Ovejero and J. Garcia, *Chem. Eng. J.*, 2016, **296**, 277–288.
49 C. Chen, D. Chen, S. Xie, H. Y. Quan, X. B. Luo and L. Guo, *ACS Appl. Mater. Interfaces*, 2017, **9**, 41043–41054.
50 F. H. Wei, D. Chen, Z. Lang, S. Q. Zhao and Y. Luo, *Dalton Trans.*, 2017, **46**, 16525–16531.
51 F. H. Wei, Q. H. Ren, D. Chen, Z. Lang, S. Q. Zhao and Y. Luo, *Nanomaterials*, 2018, **8**, 248.
52 S. Q. Zhao, D. Chen, F. H. Wei and Y. Luo, *Ultrason. Sonochem.*, 2017, **39**, 845–852.
53 X. Zhao, S. Liu, Z. Tang, H. Y. Niu, Y. Q. Cai, W. Meng, F. C. Wu and J. P. Giesy, *Sci. Rep.*, 2015, **5**, 11849.
54 Q. H. Ren, F. H. Wei, H. L Chen, D. Chen and B. Ding, *Green Process Synth*, 2021, **10**, 125–133.
55 V. T. Nguyen, T. B. Nguyen, C. W. Chen, C. M. Hung, T. D. H. Vo, J. H. Chang and C. D. Dong, *Bioresour. Technol.*, 2019, **284**, 197–203.
56 Y. Ai, Y. Liu, Y. Huo, C. F. Zhao, L. Sun, B. Han, X. R. Cao and X. K. Wang, *Environ. Sci.: Nano*, 2019, **6**, 3336–3348.
57 Z. H. Yang, J. Cao, Y. P. Chen, X. Li, W. P. Xiong, Y. Y. Zhou, C. Y. Zhou, R. Xu and Y. R. Zhang, *Microporous Mesoporous Mater.*, 2019, **277**, 277–285.